Nature Conservation 35: 41–61 (2019)
doi: 10.3897/natureconservation.35.29588
http://natureconservation.pensoft.net

RESEARCH ARTICLE

A peer-reviewed open-access journal
Nature Conservation
Launched to accelerate biodiversity conservation

The utility of Sentinel-2 Vegetation Indices (VIs) and Sentinel-1 Synthetic Aperture Radar (SAR) for invasive alien species detection and mapping

Perushan Rajah[1], John Odindi[1], Onisimo Mutanga[1], Zolo Kiala[1]

1 *Discipline of Geography, University of KwaZulu-Natal, King Edward Road, Scottsville, 3209 Pietermaritzburg, South Africa*

Corresponding author: *John Odindi* (Odindi@ukzn.ac.za)

Academic editor: *Andreas Huth* | Received 7 September 2018 | Accepted 10 April 2019 | Published 14 June 2019

http://zoobank.org/F62F8542-99C8-46E2-B25A-04F3C46A1A2A

Citation: Rajah P, Odindi J, Mutanga O, Kiala Z (2019) The utility of Sentinel-2 Vegetation Indices (VIs) and Sentinel-1 Synthetic Aperture Radar (SAR) for invasive alien species detection and mapping. Nature Conservation 35: 41–61. https://doi.org/10.3897/natureconservation.35.29588

Abstract

The threat of invasive alien plant species is progressively becoming a serious global concern. Alien plant invasions adversely affect both ecological services and socio-economic systems. Hence, accurate detection and mapping of invasive alien species is valuable in mitigating adverse ecological and socio-economic effects. Recent advances in active and passive remote sensing technology have created new and cost-effective opportunities for the application of remote sensing to invasive species mapping. In this study, new generation Sentinel-2 (S2) optical imagery was compared to S2 derived Vegetation Indices (VIs) and S2 VIs fused with Sentinel-1 (S1) Synthetic Aperture Radar (SAR) imagery for detecting and mapping the American Bramble (*Rubus cuneifolius*). Fusion of S2 VIs and S1 SAR imagery was conducted at pixel level and multi-class Support Vector Machine (SVM) image classification was used to determine the dominant land use land cover classes. Results indicated that S2 derived VIs were the most accurate (80%) in detecting and mapping Bramble, while fused S2 VIs and S1 SAR were the least accurate (54%). Findings from this study suggest that the application of S2 VIs is more suitable for Bramble detection and mapping than the fused S2 VIs and S1 SAR. The superior performance of S2 VIs highlights the value of the new generation S2 VIs for invasive alien species detection and mapping. Furthermore, this study recommends the use of freely available new generation satellite imagery for cost effective and timeous mapping of Bramble from surrounding native vegetation and other land use land cover types.

Keywords
Alien species invasions, Sentinel-1, Synthetic Aperture Radar (SAR), Sentinel-2, Vegetation Indices (VIs), American Bramble, Fusion, Support Vector Machine (SVM)

Introduction

Global biodiversity is increasingly becoming susceptible to pressure from invasive species (Butchart et al. 2010). Specifically, the rapid spread of invasive alien plants in several regions of the world has adversely impacted ecosystem health, native species diversity and local and national economies (Pysek et al. 2012; Schirmel et al. 2016; Convention on Biological Diversity 2009). Brooks et al (2006) highlight the imperative need for the protection of native biodiversity, a need further emphasised by the United Nations (UN) that declared the period between 2010 and 2020 as the decade of biodiversity (UNEP 2010). Moreover, increased costs associated with invasive alien species eradication and management programmes puts further pressure on biodiversity (Marbuah et al. 2014). The severity of the problem has increased the impetus on development of efficient and cost-effective approaches for the control and management of invasive alien plant species.

In South Africa, approximately two million hectares of land have been invaded by invasive alien plant species (van Wilgen et al. 2012). The south western, southern and eastern coastal and interior regions have been identified as highly vulnerable to invasion (Kotzé et al. 2010; van Wilgen et al. 2012; Clusella-Trullas and Garcia 2017). In KwaZulu-Natal (KZN) province, for instance, Erasmus (1984) notes that the cool and moist conditions favour a range of invasive alien plant species. The American Bramble (*Rubus cuneifolius*) has particularly thrived in the province's western mountain ranges (Henderson 2011). Originating from North America, Bramble belongs to the *Rosaceae* family and has adverse direct and indirect impacts on biodiversity that include changes in nutrient cycling, increase in soil erosion, reduction in rangeland carrying capacity and viability, as well as effects on natural plant succession, fire patterns and behaviour and hydrological processes (Henderson 2001).

To develop optimal mitigation of spread and eradication approaches, determination of spatial cover and extent of Bramble infestation is paramount. Traditionally, surveys have been adopted for mapping and monitoring of invasive alien plant species (Tan et al. 2012; Shah and Reshi 2014). However, reliance on field-based surveys is often restrictive, as they are commonly time consuming, labour and resource intensive and unsuitable in inaccessible sites. Hence, the adoption of remotely sensed imagery for invasive alien species detection and mapping has recently gained popularity. Huang and Asner (2009) attribute this increase to improved sensor technology, facilitating detailed and large scale landscape mapping and monitoring. In the recent past, the majority of invasive alien plant species detection and mapping applications have relied on remotely sensed image spatial and spectral characteristics (Mirik et al. 2013; Müllerová et al. 2013). Other studies have proposed object-based textural and contextual characteristics (Zhou et al. 2008) and landscape thermal characteristics (Eisavi et al.

2015). However, the advent of new sensors with radar scanning capabilities provides new opportunities for invasive plant species detection and mapping (Bradley 2014). For instance, radar's ability to determine surface structure and roughness, dielectric constant (moisture content) and slope angle and orientation offer great opportunities for invasive species mapping. The European Space Agency's (ESA) sentinel constellation is a recent satellite that consists of the Sentinel-1 (S1) and Sentinel-2 (S2) earth observation instruments. Both sensors disseminate freely available multispectral optical (S2) and multi-polarised SAR (S1) data. The unique S1 and S2 sensor characteristics, such as large swath widths, medium to fine scale spatial resolutions, short re-visit times and additional bands (Frampton et al. 2013; Sentinel-1 User Handbook 2012) provide numerous opportunities to evaluate the potential of the sensors to improve the reliability of remote sensing approaches for invasive alien plant species mapping.

Conventional remote sensing of invasive alien species utilises spectral wavelengths of absorbed and reflected light by distinguishing certain pigments in leaves and inflorescence (Huang and Asner 2009; Mirik et al. 2013; Weisberg et al. 2017; Müllerová et al. 2013; Bradley 2014). Hence, the potential of S2 to detect and map invasive alien species exists (Rajah et al. 2018). Specifically, the senor's improved spectral resolution can be used to derive numerous band ratios and indices, useful for vegetation mapping. For example, spectral vegetation indices (VIs), derived from remotely sensed data, have become valuable in mapping and monitoring vegetation species (Jamali et al. 2014; Zhang et al. 2015; Orhan et al. 2014). VIs have several advantages over stand-alone spectral bands that include reduced effect of atmospheric conditions, canopy geometry and shading, decreased effect of soil background on canopy reflectance and enhanced variability of spectral reflectance of target vegetation (Liu et al. 2004; Viña et al. 2011). On the other hand, the unique characteristics of S1 SAR imagery could provide additional variables that could improve invasive alien species detection and mapping. SAR data can operate at wavelengths irrespective of cloud conditions or lack of illumination and is capable of acquiring data during day and night (Sentinel-1 User Handbook 2012). SAR offers detailed information on the often difficult to detect characteristics of vegetation such as shape, moisture and roughness (Chen et al. 2010). However, despite this potential, previous adoption of SAR imagery for invasive alien plant species mapping has been limited by high acquisition cost, limited area coverage and complex data pre-processing (McNairn et al. 2009). Hence, the provision of freely available SAR imagery from the S1 satellite provides new prospects for advancing the mapping and detection of invasive alien plant species.

Asner et al. (2008) and Zhang (2010) note that the fusion of imagery from various sensors, while applying appropriate methodologies, may be valuable for invasive alien species detection and mapping. Furthermore, conventional optical imagery and SAR are commonly believed to be complimentary (Zhu et al. 2012). Considering the above-mentioned advantages, as well as S2s improved spatial, spectral and temporal characteristics valuable for generating VIs, the fusion of these datasets provides a unique opportunity to investigate the value of new generation sensors such as S1 and S2 in mapping alien species. Accordingly, this study sought to determine the performance of conventional stand-alone S2 optical imagery, stand-alone S2 derived VIs and fused S2 VIs with S1 Synthetic Aperture Radar (SAR) imagery in detecting and mapping the American Bramble.

Methodology

Study site

This study was conducted at the uKhahlamba Drakensberg Park (UDP), a UNESCO proclaimed world heritage and nature conservation area. The area is situated along the western edge of the KwaZulu-Natal province of South Africa (Figure 1). The area experiences wet and humid conditions during summer (November to March) (Nel 2009), with rainfall ranging from 990–1130 mm (Dollar and Goudy 1999). Winters (May to August) are dry and cold, with common occurrence of snow and frost (Mansour et al. 2012). Mean annual temperatures average 16° C and annual rainfall averages 1000 mm and 1800 mm at lower and higher elevations, respectively (Tyson et al. 1976). The landscape is predominantly natural grassland with wiregrass – *Aristida purpurea*, weeping lovegrass – *Eragrostis curvula* and the common thatch grass – *Hyparrhenia hirta* as dominant species. According to Everson and Everson (2016), the UDP is one of the most valuable remnant grassland in the country. The area is also characterised by patches of natural shrubs (*Erica* spp.) and isolated dense groups of bushes and trees. In the recent past, Bramble has emerged within the UDP and has invaded significant portions of the landscape (Bromilow 2010).

Field data collection

Field data collection was conducted during spring and summer of 2016. A purposive sampling technique was utilised to record ground truth points of four major land cover classes (Bare rock, Bramble, Forest and Grassland). These seasons were chosen for field data collection as Bramble patches are most phenologically discernible from native vegetation. Ground control points were recorded as close to the centroid of Bramble patches as possible. Collected Bramble patches ranged from 15 m × 15 m to 50 m × 50 m. Ground truth point data collected from Bramble patches were spatially independent from each other to compensate for the spatial resolution of the satellite imagery utilised. This ensured that each Bramble patch fell within a single image pixel and could be associated with the unique spectral reflectance of a specific pixel. Due to the area's steep and mountainous terrain, hence restricted accessibility, only Bramble patches that could be accessed by foot were considered for this study. In addition, aerial photographs at a 0.5 m spatial resolution captured in 2016 were used to supplement and verify selected land cover ground truth points. In total, 15, 40, 45 and 60 ground truth points were used for Bare rock, Forest, Grassland and Bramble, respectively.

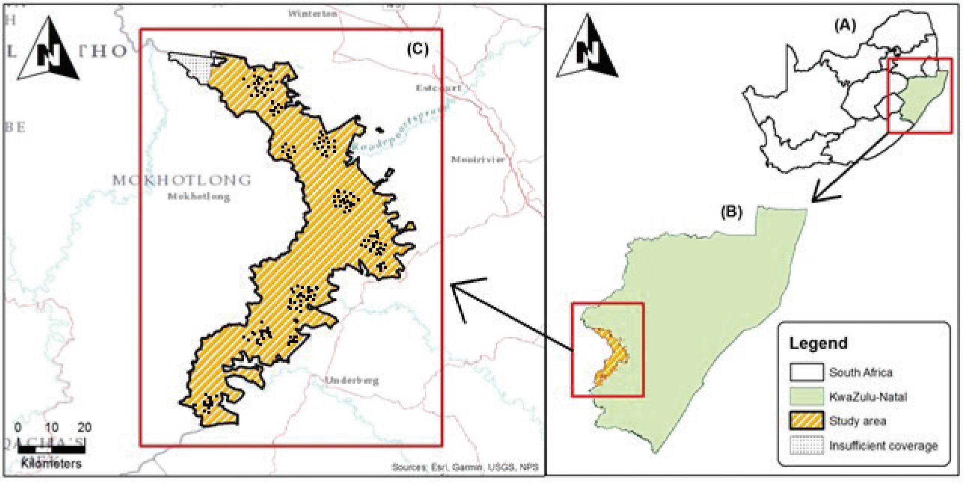

Figure 1. The uKhahlamba Drakensberg Park (UDP) (C) located within the KwaZulu-Natal Province (B) of South Africa (A) (Points within the map represent GPS cordinates of ground truth points).

Image acquisition

Optical Imagery

The Sen2Cor plugin ESA SNAP toolbox 3.0 (European Space Agency 2018) was used to convert summer Sentinel-2 level-1C raw products to surface reflectance values in the Sen2Cor plugin. Images were corrected for topographic effects to remove shadows associated with mountainous areas using the System for Automated Geoscientific Analyses SAGA (2.1.2) terrain analysis lighting tool within the Quantum GIS (QGIS) environment on a band by band basis (Conrad et al. 2015). The correction of topographic effects is a tool within the SAGA software that best adjusts optical imagery for topographic effects of shadow (Conrad et al. 2015).

Sentinel-1 Synthetic Aperture Radar (SAR) Imagery

Summer Synthetic Aperture Radar (SAR) data were downloaded from the Sentinel-1 data hub. Sentinel-1 level-1 Ground Range Detected (GRD) products were multi-looked and projected to ground range using an earth ellipsoid model. SAR Vertical-Horizontal (VH) polarised imagery was acquired using the Interferometric Wide Swath (IW) mode, with a spatial resolution of 20 metres and a 250 km^2 swath width. Pre-processing of SAR imagery was conducted using the ESA SNAP toolbox following the methodology outlined in Bevington (2016). The Bevington (2016) SAR image processing chain consists of 5 steps: (1) Application of orbit file to SAR image; (2) Radiometric calibration; (3) Terrain correction; (4) Application of speckle filter; (5)

Convert SAR DN to Gamma backscatter values. Polarisation of SAR imagery recorded in Vertical Horizontal (VH) acquisition mode was fused with S2 derived VIs. SAR backscatter measurements are believed to be a function of polarisation and target object characteristics, such as geometry, roughness and dielectric properties (Vyjayanthia and Nizalapur 2010).

Sentinel-2 derived Vegetation Indices (VIs)

Sixty-five Vegetation Indices (VIs), selected from the online Index Database (IDB) (www.indexdatabase.de), were calculated from summer Sentinel-2 surface reflectance optical imagery. The IDB is a tool developed to provide a simple overview of satellite specific vegetation indices that are usable from a specific sensor for a specific application (Henrich et al. 2009). All VIs were calculated within a python 2.7.13 environment using listed formulae from the IDB and spectral reflectance Sentinel-2 bands (Table 1). The 10 most influential VIs were selected for stand-alone classification results and subsequent image fusion with SAR imagery in order to produce a fused VIs and SAR classification result. The top 10 VI selections were determined using the Variable Importance in the Projection (VIP) method. Variable Importance in the Projection aims to improve classification accuracy by recognising a subset of all initial variables (VIs) that, if combined, could increase classification accuracies with parsimonious representation (Farrés et al. 2015; Xu et al. 2018). As aforementioned, the study area is pre-dominantly natural grassland, regarded as a valuable economic and environmental resource. Hence, in addition to Bramble, it was necessary to reliably determine the spatial extent of grassland. In this regard, the VIP was used to determine the importance of each VI in increasing the two land use land cover's user's and producer's accuracies.

Table 1. Selected S2 derived VIP vegetation indices subsequently utilized for SAR fusion

VIP Vegetation Indices (VIs)	VI formula (S2 optical bands)	
Datt2 (Simple Ratio 850/710)	Near Infrared (NIR)/Red Edge 1	Datt 1999
PSSRc2 (Simple Ratio 800/470 Pigment specific simple ratio C2)	Near Infrared (NIR)/Blue	Blackburn 1998
RDVI (Renormalized Difference Vegetation Index)	Near Infrared - Red/(Near Infrared + Red)$^{0.5}$	Roujean and Breon 1995
SR520/670 (Simple Ratio 520/670)	Blue/Red	Henrich et al. 2009
SR672/550 (Simple Ratio 672/550)	Red/Green	Henrich et al. 2009
SR800/550 (Simple Ratio 800/550)	Near Infrared/Green	Henrich et al. 2009
SR833/1649 (Simple Ratio 833/1649 MSIhyper)	Near Infrared /Shortwave Infrared1	Henrich et al. 2009
SR860/550 (Simple Ratio 860/550)	Narrow-Near Infrared/Green	Henrich et al. 2009
SRMIR/Red (Simple Ratio MIR/Red Eisenhydroxid-Index)	Shortwave Infrared2/Red Edge 1	Henrich et al. 2009
TM5/TM7 (Simple Ratio 1650/2218)	Shortwave Infrared1/ Shortwave Infrared2	Henrich et al. 2009

Image fusion

Pixel level image fusion, based on ground truth points, was used to merge the ten most influential VIP VIs and Sentinel-1 SAR imagery (a description of image fusion levels can be found in Hong et al. (2014). All VIs were derived from S2 optical bands, at a spatial resolution of 20 m. Extraction of feature pixels (ground truth points) were done separately for optical imagery (spectral reflectance measurements) and SAR imagery (backscatter measurements). Corresponding backscatter measurements were then assigned to the corresponding extracted spectral reflectance of ground truth points. Optical and SAR imagery were then fused using the composite band tool in ArcMap 10.4. This was achieved by stacking optical and SAR imagery on a band by band basis, creating a composite (fused) image containing both spectral reflectance and backscatter measurements at respective ground truth points. The fused image was then used for image analysis.

Image classification

Image classification was conducted post pixel level image fusion as outlined in Pandit and Bhiwani (2015). The Support Vector Machine (SVM) algorithm was run using the scikit-learn package in a Python environment. The SVM algorithm is a supervised statistical learning technique initially developed to handle binary classification (Vapnik 1979). SVM aims to identify a hyper-plane that is able to distinguish the input dataset into a predefined discrete number of classes consistent with training data (Mountrakis and Ogole 2011). Several evaluations of SVM have shown that the algorithm is capable of delineating several classes with a small number of support vectors as training data, without ultimately compromising classification accuracies (Foody and Mathur 2004; Mantero et al. 2005; Bruzzone et al. 2006; Shao and Lunetta 2012; Zheng et al. 2015). Spectra were extracted using ground truth points of the aforementioned major land cover classes. The fused VIP vegetation indices and SAR image measurements were used to define the SVM feature space and a radial basis kernel function used to determine optimal hyperplanes that differentiate the different land cover classes. Waske et al. (2010), for instance, established that the approach is superior to the polynomial function. Furthermore, this approach is known to be fast and computationally efficient, with a two parameter tuning requirement; cost 'sigma (C)' for error adjustment of misclassified instants of training data and kernel width 'gamma (γ)' (Waske et al. 2010). As recommended by Hsu and Lin (2002), the one-against-one approach was used to implement a multiclass-based SVM model.

Spatial cover map production and validation

Support Vector Machine classification maps were generated for S2 optical imagery, Vegetation Indices and for the fused VIS and SAR imagery within a Python environment. Training data (70%) of all four considered land cover classes were used as the input for Bramble spatial cover maps. The respective test dataset (30%) was then used to assess classification accuracies across all imagery. A confusion matrix was generated from the SVM process and user and producer accuracies used to quantify the reliability of the resultant Bramble spatial cover maps. In a confusion matrix, the overall accuracy is determined by dividing correctly classified pixels by the total number of pixels checked (Congalton and Green 1999). Two other measures, producer's and user's accuracy, can also be generated from the matrix. Producer's accuracy is determined by dividing the total number of correct pixels in one class divided by the total number of pixels as derived from reference data (Congalton and Green 1999). It is a measure of how well an area has been classified and is expressed as:

$$\textit{Producer's accuracy (\%)} = \textit{100\%} - \textit{error of omission (\%)} \tag{1}$$

User's accuracy on the other hand is a measure of map reliability and provides information on how well a map represents ground features. It is expressed as:

$$\textit{User's accuracy (\%)} = \textit{100\%} - \textit{error of commission (\%)} \tag{2}$$

Results

Sentinel-2 optical bands

The overall classification accuracy using S2 optical bands was 78% (Table 2). Bramble produced the lowest users' accuracy (46%) across all considered classes, while Grassland produced the lowest producers' accuracy (69%) (Table 3). Results produced using only S2 optical bands were used as a benchmark for classification using VIs and VIs fused with SAR imagery.

A large overestimation of Bramble discrimination and spatial cover using S2 optical bands was evident (Figures 2b and 3a). An underestimation in Grassland discrimination and spatial cover was observed, as the SVM algorithm could not effectively distinguish between Bramble and Grassland (Table 3, Figure 2b). An underestimation in the spatial cover of the Bare rock class was also evident, as there was consistent misclassification of Bare rock from Grassland and Bramble (Figures 2b and 3a).

Vegetation Indices (VIs)

Discrimination and mapping of Bramble using vegetation indices produced the highest overall accuracy (82%) when compared to the benchmark of using only S2 optical image bands (Table 3). A users' accuracy of 72% for Bramble surpassed those achieved by S2 optical imagery as well as fused vegetation indices and SAR imagery (Table 1).

Table 2. Support Vector Machine (SVM) confusion matrix using Vegetation Indices for Bramble mapping and discrimination. Where BR = Bare rock; BBL = Bramble; FR = Forest; and GR = Grassland, UA = Users accuracy; PA = Producers accuracy and OA = Overall accuracy.

S2 (Optical bands)	BR	BBL	FR	GR	UA (%)
BR	33	2	0	11	70
BBL	0	24	0	30	46
FR	1	1	51	3	92
GR	2	3	7	94	89
PA (%)	92	81	87	69	
OA (%)	**78**				

Table 3. Support Vector Machine (SVM) confusion matrix using Sentinel-2 optical bands for Bramble mapping and discrimination. Where BR = Bae rock; BBL = Bramble; FR = Forest; and GR = Grassland, UA = Users accuracy; PA = Producers accuracy and OA = Overall accuracy.

Vegetation Indices (VIs)	BR	BBL	FR	GR	UA (%)
BR	51	11	0	0	83
BBL	0	53	19	4	72
FR	1	0	54	0	97
GR	13	7	0	57	74
PA (%)	83	78	76	91	
OA (%)	**84**				

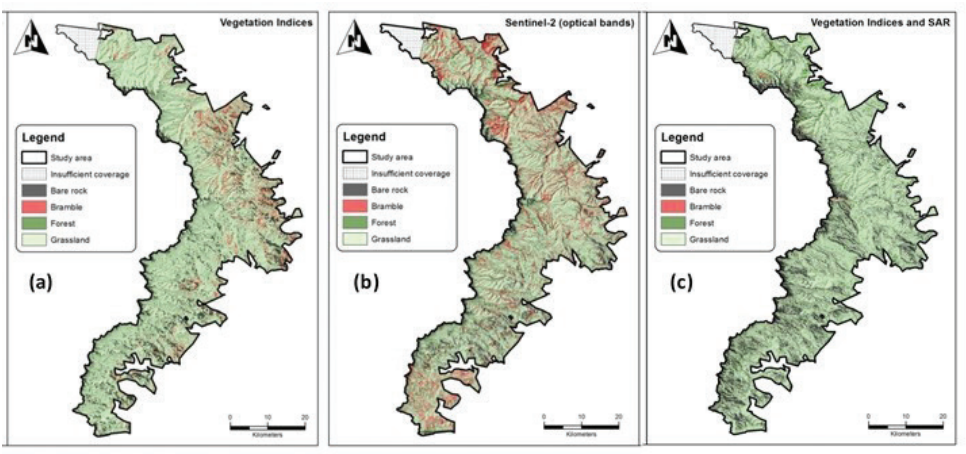

Figure 2. Support Vector Machine (SVM) classification maps produced utilising (**a**) Vegetation Indices; (**b**) S2 optical bands and (**c**) Fused VIs and SAR.

The classification map resulting from fused vegetation indices and SAR imagery showed the most accurate discrimination and spatial cover of all considered land cover classes. The Grassland and Bare rock classes were reliably discriminated (Figures 2a

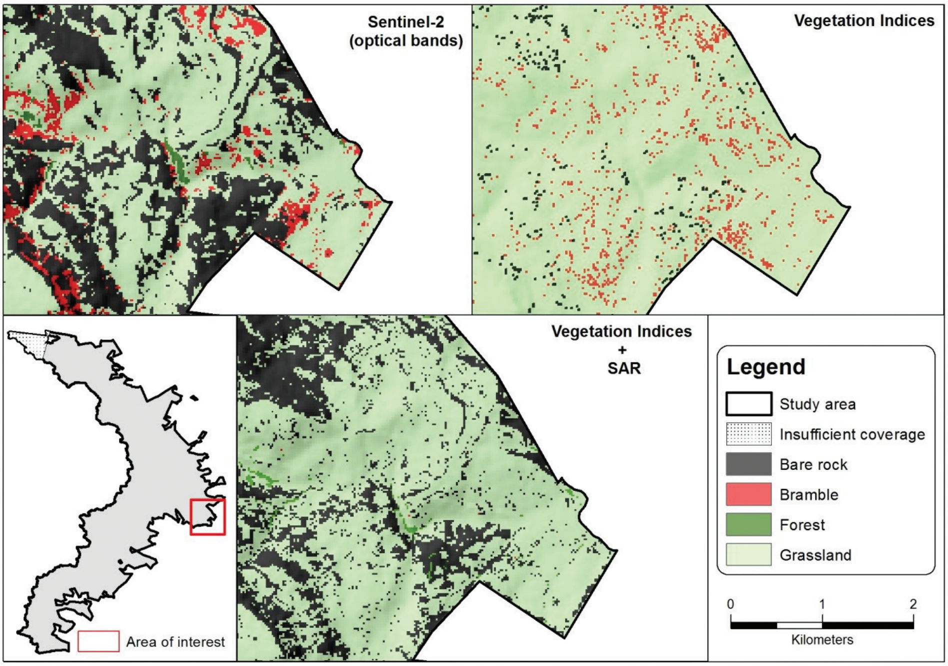

Figure 3. Overestimation and underestimation of land-cover classes within an area of interest where (**a**) = S2 optical bands; (**b**) = Vegetation indices (VIs) and (**c**) = VIs and SAR imagery.

and 3b). In addition, the spatial discrimination and cover of Bramble was reliably discriminated as compared to the S2 optical band benchmark and the fused VIs and SAR imagery (Figures 2a and 3b).

Vegetation Indices (VIs) and S1 SAR imagery

The ten most influential S2 VIs were selected for pixel level image fusion with S1 SAR imagery. Using VIP, the influence of VIs was identified by the importance on increasing Grassland and Bramble's User's and Producer's accuracy, hence, the ten bands that generated the ten highest classification accuracies were selected. Five of the selected VIs incorporated the Near Infrared (NIR) optical band, while three selected VIs were derived using Shortwave Infrared 1 (SWIR1) and Shortwave Infrared 2 (SWIR2) optical bands (Table 1). The SR520/670 and SR672/550 VIs were the only two VIP VIs derived using bands within the visible portion of the electromagnetic spectrum (Table 3).

The fusion of VIs and S1 SAR imagery produced the lowest overall accuracy (55%) when compared to the benchmark of S2 optical band results (Table 4). Bramble users' and producers' accuracies were 29% and 20%, respectively (Table 4), the lowest in all

Table 4. Support Vector Machine (SVM) confusion matrix using fused Vegetation Indices and SAR imagery for Bramble mapping and discrimination. Where BR = Bae rock; BBL = Bramble; FR = Forest; and GR = Grassland, UA = Users accuracy; PA = Producers accuracy and OA = Overall accuracy.

VIs and SAR	BR	BBL	FR	GR	UA (%)
BR	43	2	0	11	79
BBL	0	15	0	38	29
FR	1	0	45	17	73
GR	0	53	0	39	42
PA (%)	97	20	100	37	
OA (%)	**55**				

classes. The Forest (73% and 100%) and Bare rock (79% and 97%) classes were the highest users' and producers' accuracies, respectively.

The SVM classification map, produced using fused vegetation indices and SAR, resulted in an underestimation of the Bramble class, while an overestimation of the Grassland class was observed (Figure 2c). Although the Forest class received high users' and producers' accuracies, the overall distribution and discrimination were overestimated when compared to the benchmark (Figures 2c and 3c).

Discussion

This study sought to determine the potential of derived Vegetation Indices (VIs) and fused VIs and Synthetic Aperture Radar (SAR) imagery to improve invasive alien species detection and mapping. The overall classification accuracy of optical imagery was used as the benchmark for comparison of the results achieved using S2 VIs and fused VIs and SAR. Opposing the expected outcome, fused VIs and SAR imagery produced the lowest classification accuracy (55%) compared to conventional S2 optical imagery (78%). Moreover, S2 derived VIs produced the highest classification accuracy (84%) when compared to conventional S2 optical imagery and fused VIs and SAR.

Poor performance of fused VIs and SAR imagery was unanticipated and opposes research done by Sano et al. (2005), who noted that the combination of VIs and SAR for discrimination within a savannah environment was complementary and improved overall discriminant analysis. Sano et al. (2005) also noted that VIs and SAR were able to easily separate Grassland from woodlands. However, Sano et al. (2005) also reported increased confusion between Grassland and shrub species when utilising fused VIs and SAR. This provides some indication that previous studies have also encountered unanticipated results when combining VIs and SAR for discrimination purposes. Poor overall classification accuracies of fused VIs and SAR imagery can further be attributed to vegetation structure and roughness, as this plays a major role in measured SAR backscatter values. Similar difficulties were documented by Millard and Richardson (2018) who note that, even though it is well established that vegetation roughness influences

SAR backscatter, characterising these variables spatially and temporally within natural environments remains a challenge. Although results from fused VIs and SAR were unexpected, similar poor performance using the same combination of variables is not unprecedented. For example, Torma et al. (2004) also experienced poor performance when fusing VIs and SAR.

Patel et al. (2006) and Srivastava et al. (2009) note that the magnitude of SAR backscatter is dependent on SAR band frequency, for instance, SAR backscatter signatures at high frequency (e.g. X-band SAR) are known to be sensitive to subtle variations in vegetation phenology attributed to deep canopy penetration. Sentinel-1 C-band SAR is considered low frequency (decreased canopy penetration) SAR imagery and could have experienced difficulty in discerning between Bramble characteristics and surrounding native vegetation when using fused VIs and S1 SAR imagery (Khosravi et al. 2017; Duguay et al. 2015; Naidoo et al. 2015; Hajj et al. 2014; van Beijma et al. 2014; Turkar et al. 2012). The influence of sensor incident angle on SAR backscatter is known to be interpreted using the same mechanism, particularly for lower frequencies of SAR. Inoue et al. (2002) notes that correlations to plant physiological characteristics, such as Leaf Area Index (LAI), canopy height and stem density, decrease with an increasing incident angle. This is mainly attributed to the penetration of SAR microwaves responsible for backscatter measurements, as smaller incident angles are able to penetrate deeper into canopy cover, hence extract more physiological information (McNairn et al. 2009). The relatively large incident angle of S1 (46°) (Sentinel-1 User Handbook 2012) could have hindered its ability to distinguish vegetation physiological information, which could serve to justify decreased classification accuracies achieved using fused VIs and SAR imagery (de Almeida Furtado et al. 2016; Naidoo et al. 2015; Frampton et al. 2013; Vyjayanthia and Nizalapur 2010). The influence of soil moisture and roughness on leaf and stalk SAR backscatter measurements is considered a weakness of SAR imagery across specific classification applications (Moran et al. 2002). SAR imagery could have served to increase confusion between Bramble and surrounding native vegetation when fused with S2 VIs.

The use of S2 VIs outperformed the benchmark accuracy achieved by conventional S2 optical imagery. Similar results were achieved by Kandwal et al. (2009), where selected VIs performed well in discriminating Lantana camara (*Verbenaceae*), an invasive alien plant with similar growth pattern and phenology to Bramble. The majority of Vis, selected as VIP indices, were dominated by VIs incorporating the Near Infrared (NIR), Shortwave Infrared (SWIR) and red edge S2 bands. A study by Zhao et al. (2007) produced similar results, where VIs, derived from SWIR, red-edge and NIR bands, were reported to be closely correlated to canopy LAI and canopy chlorophyll density. Chuai et al. (2013), for instance, used NDVI to determine seasonal vegetation correlations with lag-time climatic effects in Inner Mongolia between 1998 and 2007. They established varied seasonal changes and concluded that NDVI provides a reliable measure of vegetation changes attributed to climatic variability. According to Domaç et al. (2004), VIs can extract valuable information by generating a new variable set without inter-band correlation and reduced data dimensionality. Whereas the NDVI has commonly been preferred in vegetation mapping, El-Mezouar et al. (2010) suggests that Soil Adjusted Vegetation Index (SAVI) is more suitable for mapping patchy vegetation characterised by lower percentage cover. A recent study by Tarantino et al. (2019) in Apulia region, southern Italy, concluded that indices like MSAVI on WorldView2 imagery are effective in discriminating the invasive *Aillanthus aitissina* species. This superior performance is attributed to the indices' maximal reduction of background soil effect on vegetation reflectance (Qi et al. 1994). Other studies like Groβe-Stoltenbeg et al. (2018) used 15 vegetation indices to determine an *Acacia lonifolia* cove in a dune ecosystem and concluded that the fusion of vegetation indices with LIDAR could effectively determine the effects of species invasion on the dune landscape.

Eight of the ten VIP VIs selected for Bramble discrimination and mapping were derived from at least one of these three spectral bands. The strong relationship between NIR, SWIR and red edge bands to variable vegetation parameters could have resulted in the increased accuracy of Bramble discrimination and mapping. Moreover, reflectance within the visible region of the spectrum is largely determined by vegetation pigments and is commonly used to quantify vegetation physiological properties (Li et al. 2013; Zhao et al. 2007). The collective capability of combined VIs to discriminate various vegetation parameters could further explain the increased overall classification accuracy achieved using stand-alone vegetation indices.

Several studies (e.g. Royimani et al (in press) – *Perthenium*, Matongera et al. (2017) - *Pteridium aquilinum* (L.) *Kuhn*, Robinson et al. (2016) - *Mesquite* (*prosopts* spp.), Peters et al. (1992) - *Gutierrezia sarothrae* and Oumar (2016) - *Lantana camara* have discriminated invasive species from native vegetation using spectral variability. Matongera et al. (2017) and Zhao et al. (2009) attribute this to invasive species' dissimilar biophysical (e.g. texture, canopy, leaf structure and orientation) and biochemical (e.g. chlorophyll and water content) characteristics from the surrounding vegetation species. According to Blossey and Notzold (1995), invasive species are commonly characterised by superior physical development due to disproportionate availability or exploitation of resources. Such differences, particularly volume and height, facilitate their discrimination. Goodwin et al. (1999), for instance, noted that differences in stem heights and flowering periods could be used to discriminate invasive species from native vegetation, while Peerbhay et al. (2016) found that dense infestation, particularly in new habitats, facilitate discrimination. Commonly, the phenology of invasive species differs from native plants. Holland and Aplin (2013) and Page (2010) note that the discreet reflectance of invasive species at different seasons offers great potential for their discrimination. This is consistent with Santos and Ustin (2018) who noted that fennel (*Foeniculum vulgare*) could be effectively discriminated by considering seasonal foliar variability from surrounding grasses. In this study, Bramble's broad leafs could have facilitated its discrimination, a finding in agreement with Hong et al. (2014) who successfully discriminated alfalfa in the Prairie Provinces of Canada.

According to Motohka et al. (2010), the potential of green-red VIs for phenological vegetation discrimination exists. VIs derived from ratios of red and green optical bands are known to be sensitive to variations in canopy colour, where changes in visible characteristics of vegetation canopy are often timeously detected (Motohka et al. 2010). The SR672/550 VI, an index derived solely from S2 red and green optical bands, suggests an agreement with Motohka et al. (2010). The SR672/550 VI could have assisted in the discrimination of Bramble as it produces noticeable white inflorescence during summer, a significant phenological trait that could have been exploited. This potential is further enhanced by S2's higher temporal resolution (five days, with possible higher resolution due to overlap in swaths of adjacent orbits) that facilitates single scene's image turnover. Although the combined potential of VIs and SAR imagery produced the lowest overall classification accuracy, the potential of the latest and advanced spectrally derived VIs was evident when compared to the benchmark set by conventional S2 optical imagery. While the fusion of S2 VIs and SAR showed limited utility with regard to accurately mapping Bramble, the complementarity of these datasets has previously been documented. Our findings are consistent with existing literature. For instance, in lower Magdalena region, Colombia, Clerici (2017) established that Sentinel 1 and 2 fused dataset, classified using SVM, generated the highest classification accuracy of the existing land use land covers. Hence, the study recommended the use of radar sensor due to its all-weather capability and the spectral wealth of the optical sensor. Niculescu et al. (2018) mapped major vegetation types by fusing S1, S2 and SPOT – 6 in Pays de Brest, France by stacking time series data using Random Forest supervised classification. The study achieved a 93% classification accuracy when the major vegetation indices (Normalised Difference Vegetation Index - NDVI, Normalised Difference Wetness Index NDWI, Inverted Red-Edge Chlorophyll Index - IRECI and Sentinel-2 Red-Edge Position - S2REP) were used in the classification process. The study recommends the use of S1 and S2 due to free availability and improved sensor capabilities.

Conclusion

This study utilised freely available advanced Sentinel-1 radar and Sentinel-2 optical imagery, with the aim of evaluating spectrally derived VIs and fusing Synthetic Aperture Radar (SAR) imagery for improving American Bramble (*Rubus cuneifolius*) detection and mapping. This study contributes to the evaluation of economically viable, efficient and large scale invasive alien species detection and mapping. Conventional S2 optical imagery was used as a benchmark for comparison with results achieved using S2 VIs and fused VIs and S1 SAR imagery. The use of S2 VIs increased overall classification accuracies when compared to traditional optical imagery results, while the fusion of S2 VIs and S1 SAR decreased the overall accuracies. Hence this study demonstrated that new generation S2 VIs have the potential to increase the detection and mapping of Bramble from surrounding native vegetation. Results further indicate that the fusion of VIs and SAR imagery for Bramble detection and mapping failed to increase overall classification accuracies, hence have limited utility when applied to Bramble detection and mapping. The new generation satellites, such as S1 and S2, possess unprecedented sensor characteristics like higher temporal and spatial resolution, as well as tandem acquisition of SAR data, hence valuable for improved landscape mapping. This study concludes that the recently launched Sentinel satellite, with optical and radar capabilities, holds great promise in landscape delineation and vegetation mapping.

References

Asner GP, Knapp DE, Kennedy-Bowdoin T, Jones MO, Martin RE, Boardman J, Hughes RF (2008) Invasive species detection in Hawaiian rainforests using airborne imaging spectroscopy and LiDAR. Remote Sensing of Environment 112(5): 1942–1955. https://doi.org/10.1016/j.rse.2007.11.016

Bevington A (2016) Polarimetric Synthetic Aperture Radar (InSAR) analysis of Prince George UNBC Remote Sensing Lab, 2016.

Blossey B, Notzold R (1995) Evolution of increased competitive ability in invasive non-indigenous plants: A hypothesis. Journal of Ecology 83(5): 887–889. https://doi.org/10.2307/2261425

Bradley B (2014) Remote detection of invasive plants: A review of spectral, textural and phenological approaches. Biological Invasions 16(7): 1411–1425. https://doi.org/10.1007/s10530-013-0578-9

Bromilow C (2010) Problem plants and alien weeds of South Africa. Briza Publications, Pretoria.

Brooks TM, Mittermeier RA, da Fonseca GAB, Gerlach J, Hoffmann M (2006) Global biodiversity conservation priorities, Science 313:58–61. https://doi.org/10.1126/science.1127609

Bruzzone L, Chi M, Marconcini M (2006) A novel transductive SVM for semisupervised classification of remote-sensing images. IEEE Transactions on Geoscience and Remote Sensing 44(11): 3363–3373. https://doi.org/10.1109/TGRS.2006.877950

Butchart SH, Walpole M, Collen B, Van Strien A, Scharlemann JP, Almond RE, Baillie JE, Bomhard B, Brown C, Bruno J, Carpenter KE (2010) Global biodiversity: Indicators of recent declines. Science 1187512. https://doi.org/10.1126/science.1187512

Chen S, Zhang R, Su H, Tian J, Xia J (2010) SAR and multispectral image fusion using generalized IHS transform based on à trous wavelet and EMD decompositions. IEEE Sensors Journal 10(3): 737–745. https://doi.org/10.1109/JSEN.2009.2038661

Chuai XW, Huang XJ, Wanga WJ, Bao G (2013) NDVI, temperature and precipitation changes and their relationships with different vegetation types during 1998–2007 in Inner Mongolia, China. International Journal of Climatology 33(7): 1696–1706. https://doi.org/10.1002/joc.3543

Clerici N, Augusto C, Calderon V, Posada J (2017) Fusion of Sentinel-1A and Sentinel-2A data for land cover mapping: A case study in the lower Magdalena region, Colombia. Journal of Maps 13(2): 718–726. https://doi.org/10.1080/17445647.2017.1372316

Clusella-Trullas S, Garcia RA (2017) Impacts of invasive plants on animal diversity in South Africa: A synthesis. Bothalia-African Biodiversity & Conservation 47: 1–12. https://doi.org/10.4102/abc.v47i2.2166

Congalton RG, Green K (1999) Assessing the Accuracy of Remotely Sensed Data Principles and Practices. Lewis Publishers, Boca Raton. https://doi.org/10.1201/9781420048568

Conrad O, Bechtel B, Bock M, Dietrich H, Fischer E, Gerlitz L, Wehberg J, Wichmann V, Böhner J (2015) System for Automated Geoscientific Analyses (SAGA) v. 2.1.4. Geoscientific Model Development 8(7): 1991–2007. https://doi.org/10.5194/gmd-8-1991-2015
Convention on Biological Diversity (2009) Strategic Plan for Biodiversity 2011-2020 and the Aichi Targets, Convention on Biological Diversity, United Nations, Montreal, Quebec.
Datt B (1999) Visible/near infrared reflectance and chlorophyll content in Eucalyptus leaves. International Journal of Remote Sensing 20(14): 2741–2759. https://doi.org/10.1080/014311699211778
de Almeida Furtado LF, Silva TSF, de Moraes Novo EML (2016) Dual-season and full-polarimetric C band SAR assessment for vegetation mapping in the Amazon várzea wetlands. Remote Sensing of Environment 174: 212–222. https://doi.org/10.1016/j.rse.2015.12.013
Dollar E, Goudy A (1999) Environmental Change: The Geography of South Africa in a Changing World. Oxford University Press, Oxford.
Domaç A, Zeydanli U, Yeşilnacar E, Süzen L (2004) Integration and usage of indices, feature components and topography in vegetation classification for regional biodiversity assessment. http://www.cartesia.org/geodoc/isprs2004/comm7/papers/39.pdf
Duguay Y, Bernier M, Lévesque E, Tremblay B (2015) Potential of C and X band SAR for shrub growth monitoring in sub-arctic environments. Remote Sensing 7(7): 9410–9430. https://doi.org/10.3390/rs70709410
Eisavi V, Homayouni S, Yazdi A, Alimohammadi A (2015) Land cover mapping based on random forest classification of multitemporal spectral and thermal images. Environmental Monitoring and Assessment, 187: 291–305. https://doi.org/10.1007/s10661-015-4489-3
El-Mezouar MC, Taleb N, Kpalma K, Ronsin J (2010) A high-resolution index for vegetation extraction in IKONOS images. SPIE. Proceedings of the SPIE on Remote Sensing for Agriculture, Ecosystems, and Hydrology, Sep 2010, Toulouse, France. SPIE, 7824 (XII), 78242A-1–78242A-9. https://doi.org/10.1117/12.866187
Erasmus DJ (1984) Bramble Farming in South Africa, Weeds, A.3/1984.Department of Agriculture and Water Supply, Pretoria.
European Space Agency (2018) Step Science toolbox exploitation platform. http://step.esa.int/main/toolboxes/snap
Everson CS, Everson T (2016) The long-term effects of fire regime on primary production of montane grasslands in South Africa. African Journal of Range & Forage Science 33(1): 33–41. https://doi.org/10.2989/10220119.2015.1124922
Farrés M, Platikanov S, Tsakovski S, Tauler R (2015) Comparison of the variable importance in projection (VIP) and of the selectivity ratio (SR) methods for variable selection and interpretation. Journal of Chemometrics 29(10): 528–536. https://doi.org/10.1002/cem.2736
Foody GM, Mathur A (2004) Toward intelligent training of supervised image classifications: Directing training data acquisition for SVM classification. Remote Sensing of Environment 93(1–2): 107–117. https://doi.org/10.1016/j.rse.2004.06.017
Frampton WJ, Dash J, Watmough G, Milton EJ (2013) Evaluating the capabilities of Sentinel-2 for quantitative estimation of biophysical variables in vegetation. ISPRS Journal of Photogrammetry and Remote Sensing 82: 83–92. https://doi.org/10.1016/j.isprsjprs.2013.04.007

Goodwin BJ, McAllister AJ, Fahrig L (1999) Predicting invasiveness of plant species based on biological information. Conservation Biology 13(2): 422–426. https://doi.org/10.1046/j.1523-1739.1999.013002422.x

Groβe-Stoltenbeg A, Hellmann C, Thiele J, Werner C, Oldeland J (2018) Early detection of GPP-related regime shifts after plant invasion by integrating imaging spectroscopy with airborne LiDAR. Remote Sensing of Environment 209: 780–792. https://doi.org/10.1016/j.rse.2018.02.038

Hajj ME, Baghdadi N, Belaud G, Zribi M, Cheviron B, Courault D, Hagolle O, Charron F (2014) Irrigated grassland monitoring using a time series of terraSAR-X and COSMO-skyMed X-Band SAR Data. Remote Sensing 6: 0002-10032. https://doi.org/10.3390/rs61010002

Henderson L (2001) Alien Weeds and Invasive Plants: A Complete Guide to Declared Weeds and Invaders in South Africa. Plant Protection Research Institute, Agricultural Research Council, Pretoria.

Henderson L (2011) SAPIA News, Southern African Plant Invaders Atlas, Agricultural Research Council - Plant Protection Research Institute, 19, Pretoria. https://doi.org/10.4001/003.019.0207

Henrich V, Jung A, Götze C, Sandow C, Thürkow D, Gläßer C (2009) Development of an online indices database: Motivation, concept and implementation. 6th EARSeL Imaging Spectroscopy.

Holland J, Aplin P (2013) Super-resolution image analysis as a means of monitoring bracken (*Pteridium aquilinum*) distributions. ISPRS Journal of Photogrammetry and Remote Sensing 75: 48–63. https://doi.org/10.1016/j.isprsjprs.2012.10.002

Hong G, Zhang A, Zhou F, Brisco B (2014) Integration of optical and synthetic aperture radar (SAR) images to differentiate grassland and alfalfa in Prairie area. International Journal of Applied Earth Observation and Geoinformation, 28 (1): 12–19. https://doi.org/10.1016/j.jag.2013.10.003

Hsu CW, Lin CJ (2002) A Comparison of Methods for Multiclass Support Vector Machines. IEEE Transactions on Neural Networks 13(2): 415–425. https://doi.org/10.1109/72.991427

Huang C, Asner GP (2009) Applications of Remote Sensing to Alien Invasive Plant Studies. Sensors (Basel) 9(6): 4869–4889. https://doi.org/10.3390/s90604869

Inoue Y, Kurosu T, Maeno H, Uratsuka S, Kozu T, Dabrowska-Zielinska K, Qi J (2002) Season-long daily measurements of multifrequency (Ka, Ku, X, C, and L) and full-polarization backscatter signatures over paddy rice field and their relationship with biological variables. Remote Sensing of Environment 81(2–3): 194–204. https://doi.org/10.1016/S0034-4257(01)00343-1

Jamali S, Seaquist J, Eklundh L, Ardö J (2014) Automated mapping of vegetation trends with polynomials using NDVI imagery over the Sahel. Remote Sensing of Environment 141: 79–89. https://doi.org/10.1016/j.rse.2013.10.019

Kandwal R, Jeganathan C, Tolpekin V, Kushwaha SPS (2009) Discriminating the invasive species, 'Lantana' using vegetation indices. Photonirvachak (Dehra Dun) 37(2): 275–290. https://doi.org/10.1007/s12524-009-0027-5

Khosravi I, Safari A, Homayouni S (2017) Separability analysis of multifrequency SAR polarimetric features for land cover classification. Remote Sensing Letters 8(12): 1152–1161. https://doi.org/10.1080/2150704X.2017.1365386

Kotzé JDF, Beukes H, van der Beg E, Newby T (2010) National Invasive Alien Plant Survey – Dataset, Agricultural Research Council: Institute for Soil, Climate and Water, Pretoria.

Li P, Jiang L, Feng Z (2013) Cross-comparison of vegetation indices derived from Landsat-7 enhanced thematic mapper plus (ETM+) and Landsat-8 operational land imager (OLI) sensors. Remote Sensing 6(1): 310–329. https://doi.org/10.3390/rs6010310

Liu Y, Zha Y, Gao J, Ni S (2004) Assessment of grassland degradation near Lake Qinghai, West China, using Landsat TM and in situ reflectance spectra data. International Journal of Remote Sensing 25(20): 4177–4189. https://doi.org/10.1080/01431160410001680419

Mansour K, Mutanga O, Everson T, Adam E (2012) Discriminating indicator grass species for rangeland degradation assessment using hyperspectral data resampled to AISA Eagle resolution. ISPRS Journal of Photogrammetry and Remote Sensing 70: 56–65. https://doi.org/10.1016/j.isprsjprs.2012.03.006

Mantero P, Moser G, Serpico SB (2005) Partially supervised classification of remote sensing images through SVM-based probability density estimation. IEEE Transactions on Geoscience and Remote Sensing 43(3): 559–570. https://doi.org/10.1109/TGRS.2004.842022

Marbuah G, Gren I, McKie B (2014) Economics of Harmful Invasive Species: A Review. Diversity (Basel) 6(3): 500–523. https://doi.org/10.3390/d6030500

Matongera TN, Mutanga O, Dube T, Sibanda M (2017) Detection and mapping the spatial distribution of bracken fern weeds using the Landsat 8 OLI new generation sensor. International Journal of Applied Earth Observation and Geoformation 57: 93–103. https://doi.org/10.1016/j.jag.2016.12.006

McNairn H, Champagne C, Shang J, Holmstrom D, Reichert G (2009) Integration of optical and Synthetic Aperture Radar (SAR) imagery for delivering operational annual crop inventories. ISPRS Journal of Photogrammetry and Remote Sensing 64(5): 434–449. https://doi.org/10.1016/j.isprsjprs.2008.07.006

Millard K, Richardson M (2018) Quantifying the relative contributions of vegetation and soil moisture conditions to polarimetric C-Band SAR response in a temperate peatland. Remote Sensing of Environment 206: 123–138. https://doi.org/10.1016/j.rse.2017.12.011

Mirik M, Ansley RJ, Steddom K, Jones DC, Rush CM, Michels Jr GJ, Elliott NC (2013) Remote distinction of a noxious weed (musk thistle: Carduusnutans) using airborne hyperspectral imagery and the support vector machine classifier. Remote Sensing 5(2): 612–630. https://doi.org/10.3390/rs5020612

Moran MS, Hymer DC, Qi J, Kerr Y (2002) Comparison of ERS-2 SAR and Landsat TM imagery for monitoring agricultural crop and soil conditions. Remote Sensing of Environment 79(2–3): 243–252. https://doi.org/10.1016/S0034-4257(01)00276-0

Motohka T, Nasahara KN, Oguma H, Tsuchida S (2010) Applicability of green-red vegetation index for remote sensing of vegetation phenology. Remote Sensing 2(10): 2369–2387. https://doi.org/10.3390/rs2102369

Mountrakis GJ, Ogole C (2011) Support vector machines in remote sensing: A review. ISPRS Journal of Photogrammetry and Remote Sensing 66(3): 247–259. https://doi.org/10.1016/j.isprsjprs.2010.11.001

Müllerová J, Pergl J, Pyšek P (2013) Remote sensing as a tool for monitoring plant invasions: Testing the effects of data resolution and image classification approach on the detection of a model plant species Heracleum mantegazzianum (giant hogweed). International Journal of Applied Earth Observation and Geoinformation 25: 55–65. https://doi.org/10.1016/j.jag.2013.03.004

Naidoo L, Mathieu R, Main R, Kleynhans W, Wessels K, Asner G, Leblon B (2015) Savannah woody structure modelling and mapping using multi-frequency (X-, C-and L-band) Synthetic Aperture Radar data. ISPRS Journal of Photogrammetry and Remote Sensing 105: 234–250. https://doi.org/10.1016/j.isprsjprs.2015.04.007

Nel W (2009) Rainfall trends in the KwaZulu-Natal Drakensberg region of South Africa during the twentieth century. International Journal of Climatology, 29: 1634–1641. https://doi.org/10.1002/joc.1814

Niculescu S, Billey A, Talab-Ou-Ali A (2018) Random forest classification using Sentinel-1 and Sentinel – 2 series for vegetation monitoring in Pay de Brest (France), Proceedings of SPIE 10783, Remote Sensing for Agriculture, Ecosystems and Hydrology XX, 1078305, 9th Oct 2018. https://doi.org/10.1117/12.2325546

Orhan O, Ekercin S, Dadaser-Celik F (2014) Use of Landsat Land Surface Temperature and Vegetation Indices for Monitoring Drought in the Salt Lake Basin Area, Turkey. The Scientific World Journal, Article ID 142939, 11 pages. https://doi.org/10.1155/2014/142939

Oumar Z (2016) Assessing the utility of the spot 6 sensor in detecting and mapping Lantana camara for a community clearing project in KwaZulu-Natal, South Africa. South African Journal of Geomatics 5(2): 214–226. https://doi.org/10.4314/sajg.v5i2.9

Page CN (2010) The Ferns of Britain and Ireland. Cambridge University, Press

Pandit VR, Bhiwani RJ (2015) Image fusion in remote sensing applications: A review. International Journal of Computers and Applications 120(10): 22–33. https://doi.org/10.5120/21263-3846

Patel P, Srivastava HS, Panigrahy S, Parihar JS (2006) Comparative evaluation of the sensitivity of multi-polarized multi-frequency SAR backscatter to plant density. International Journal of Remote Sensing 27(2): 293–305. https://doi.org/10.1080/01431160500214050

Peerbhay K, Mutanga O, Lottering R, Bangamwabo V, Ismail R (2016) Detecting bugweed (Solanum mauritianum) abundance in plantation forestry using multisource remote sensing. ISPRS Journal of Photogrammetry and Remote Sensing 121: 167–176. https://doi.org/10.1016/j.isprsjprs.2016.09.014

Peters AJ, Reed BC, Eve MD, McDaniel K (1992) Remote Sensing of Broom Snakeweed (Gutierrezia Sarothrae) with NOAA-10 Spectral Image Processing. Weed Technology 6(04): 1015–1020. https://doi.org/10.1017/S0890037X00036642

Qi J, Chehbouni A, Huete AR, Kerr YH, Sorooshian S (1994) Modified Soil Adjusted Vegetation Index (MSAVI). Remote Sensing of Environment 48(2): 119–126. https://doi.org/10.1016/0034-4257(94)90134-1

Rajah P, Odindi J, Mutanga O (2018) Evaluating the potential of freely available multispectral remotely sensed imagery in mapping American Bramble (Rubus cuneifolius). The South African Geographical Journal 100(3): 291–307. https://doi.org/10.1080/03736245.2018.1461683

Robinson T, Wardell-Johnson G, Pracilio G, Brown C, Corner R, Van Klinken R (2016) Testing the discrimination and detection limits of WorldView-2 imagery on a challenging invasive plant target. International Journal of Applied Earth Observation and Geoinformation 44: 23–30. https://doi.org/10.1016/j.jag.2015.07.004

Royimani L, Mutanga O, Odindi J, Dube T, Matonger T (in press) Advancements in satellite remote sensing for mapping and monitoring of alien invasive plant species (AIPs). Physics and Chemistry of the Earth.

Sano EE, Ferreira LG, Huete AR (2005) Synthetic aperture radar (L band) and optical vegetation indices for discriminating the Brazilian savanna physiognomies: A comparative analysis. Earth Interactions 9(15): 1–15. https://doi.org/10.1175/EI117.1

Schirmel J, Bundschuh M, Entling MH, Kowarik I, Buchholz S (2016) Impacts of invasive plants on resident animals across ecosystems, taxa, and feeding types: A global assessment. Global Change Biology 22(2): 594–603. https://doi.org/10.1111/gcb.13093

Sentienl-1 User Handbook (2012) European Space Agency. Accessed on 23/2/2019 from https://sentinel.esa.int/documents/247904/349449/S1_SP-1322_1.pdf

Shah MA, Reshi ZA (2014) Characterization of alien aquatic flora of Kashmir Himalaya: Implications for invasion management. Tropical Ecology 55: 143–157.

Shao Y, Lunetta RS (2012) Comparison of support vector machine, neural network, and CART algorithms for the land-cover classification using limited training data points. ISPRS Journal of Photogrammetry and Remote Sensing 70: 78–87. https://doi.org/10.1016/j.isprsjprs.2012.04.001

Srivastava HS, Patel P, Sharma Y, Navalgund RR (2009) Multi-frequency and multi-polarized SAR response to thin vegetation and scattered trees. Current Science 2009: 97.

Tan DT, Thu PQ, Dell B (2012) Invasive Plant Species in the National Parks of Vietnam. Forests 3(4): 997–1016. https://doi.org/10.3390/f3040997

Tarantino C, Casellab F, Adamo M, Lucas R, Beierkuhnlein C, Blonda P (2019) *Ailanthus altissima* mapping from multi-temporal very high resolution satellite images. ISPRS Journal of Photogrammetry and Remote Sensing 147: 90–103. https://doi.org/10.1016/j.isprsjprs.2018.11.013

Torma M, Lumme J, Patrikainen N, Luojus K (2004) Fusion of low resolution optical and high resolution SAR data for land cover classification. In Geoscience and Remote Sensing Symposium, IGARSS'04. Proceedings. 2004 IEEE International, 2680–2683. https://doi.org/10.1109/IGARSS.2004.1369852

Turkar V, Deo R, Rao YS, Mohan S, Das A (2012) Classification accuracy of multi-frequency and multi-polarization SAR images for various land covers. IEEE Journal of Selected Topics in Applied Earth Observations and Remote Sensing 5(3): 936–941. https://doi.org/10.1109/JSTARS.2012.2192915

Tyson PD, Preston-Whyte RA, Schulze RE (1976) The climate of the Drakensberg, Natal Town and regional planning report, 31.

UNEP (2010) Strategic Plan for Biodiversity 2011–2020 and the Aichi Targets. Accessed from https://www.cbd.int/doc/strategic-plan/2011-2020/Aichi-Targets-EN.pdf

Santos M, Ustin SL (2018) Spectral identification of native and non-native plant species. Proceedings of ASD and IEEEGRS; Art, Science and Applications of Reflectance Spectroscopy Symposium. https://doi.org/10.1109/IGARSS.2018.8517397

van Beijma S, Comber A, Lamb A (2014) Use of airborne polarimetric SAR, optical and elevation data for mapping and monitoring of salt marsh vegetation habitats. In: SAR Image Analysis, Modeling, and Techniques XIV, International Society for Optics & Photonics, 9243. https://doi.org/10.1117/12.2066487 van Wilgen BW, Forsyth GG, Le Maitre DC, Wannenburgh A, Kotzé JD, van den Berg E, Henderson L (2012) An assessment of the effectiveness of a large, national-scale invasive alien plant control strategy in South Africa. Biological Conservation 148(1): 28–38. https://doi.org/10.1016/j.biocon.2011.12.035

Vapnik V (1979) Estimation of Dependencies Based on Empirical Data. Nauka, Moscow.

Viña A, Gitelson AA, Nguy-Robertson AL, Peng Y (2011) Comparison of different vegetation indices for the remote assessment of green leaf area index of crops. Remote Sensing of Environment 115(12): 3468–3478. https://doi.org/10.1016/j.rse.2011.08.010

Vyjayanthia N, Nizalapur V (2010) Synthetic Aperture radar data analysis for vegetation classification and biomass estimation of tropical forest area. PhD Thesis, Jawaharlal Nehru Technological University. [unpublished]

Waske BJ, Benediktsson A, Árnason K, Sveinsson JR (2010) Mapping of Hyperspectral AVIRIS Data Using Machine-Learning Algorithms. Canadian Journal of Remote Sensing 35(sup1, S1): S106–S116. https://doi.org/10.5589/m09-018

Weisberg PJ, Dilts TE, Baughman OW, Meyer SE, Leger EA, Van Gunst KJ, Cleeves L (2017) Development of remote sensing indicators for mapping episodic die-off of an invasive annual grass (Bromus tectorum) from the Landsat archive. Ecological Indicators 79: 173–181. https://doi.org/10.1016/j.ecolind.2017.04.024

Xu S, Lu B, Baldea M, Edgar T, Nixon M (2018) An improved variable selection method for support vector regression in NIR spectral modelling. Journal of Process Control 67: 83–93. https://doi.org/10.1016/j.jprocont.2017.06.001

Zhang J (2010) Multi-source remote sensing data fusion: Status and trends. International Journal of Image and Data Fusion 1(1): 5–24. https://doi.org/10.1080/19479830903561035

Zhang G, Xiao X, Dong J, Kou W, Jin C, Qin Y, Zhou Y, Wang J, Menarguez M, Biradar C (2015) Mapping paddy rice planting areas through time series analysis of MODIS land surface temperature and vegetation index data. ISPRS Journal of Photogrammetry and Remote Sensing 106: 157–171. https://doi.org/10.1016/j.isprsjprs.2015.05.011

Zhao D, Huang L, Li J, Qi J (2007) A comparative analysis of broadband and narrowband derived vegetation indices in predicting LAI and CCD of a cotton canopy. ISPRS Journal of Photogrammetry and Remote Sensing 62(1): 25–33. https://doi.org/10.1016/j.isprsjprs.2007.01.003

Zhao B, Yan Y, Guo H, He M, Gu Y, Li B (2009) Monitoring rapid vegetation succession in estuarine wetland using time series MODIS-based indicators: An application in the Yangtze River Delta area. Ecological Indicators 9(2): 346–356. https://doi.org/10.1016/j.ecolind.2008.05.009

Zheng B, Myint SW, Thenkabail PS, Aggarwal RM (2015) A support vector machine to identify irrigated crop types using time-series Landsat NDVI data. International Journal of Applied Earth Observation and Geoinformation 34: 103–112. https://doi.org/10.1016/j.jag.2014.07.002

Zhou W, Troy A, Grove M (2008) Object-based Land Cover Classification and Change Analysis in the Baltimore Metropolitan Area Using Multitemporal High Resolution Remote Sensing Data. Sensors, 8(3): 1613–1636. https://doi.org/10.3390/s8031613

Zhu Z, Woodcock CE, Rogan J, Kellndorfer J (2012) Assessment of spectral, polarimetric, temporal, and spatial dimensions for urban and peri-urban land cover classification using Landsat and SAR data. Remote Sensing of Environment 117: 72–82. https://doi.org/10.1016/j.rse.2011.07.020